Electronic Supplementary Information

Fluorescent Probes for Formaldehyde based on Formaldehyde-promoted C-N Cleavage of Azanyl Carbamates

Wanjin Xing,[a] Yang Li,[a] Yulin Que,[a] Huan Xu,*[b] Wei Wang,*[c] and Kaiyan Lou*[a]

[a] State Key Laboratory of Bioreactor Engineering, Shanghai Frontiers Science Center of Optogenetic Techniques for Cell Metabolism, Shanghai Key Laboratory of New Drug Design, and Shanghai Key Laboratory of Chemical Biology, School of Pharmacy, East China University of Science & Technology, 130 Meilong Road, Shanghai 200237, China.
[b] School of Public Health, Anhui University of Science and Technology, Hefei, Anhui Province, 231131, China.
[c] Department of Pharmacology and Toxicology and BIO5 Institute, University of Arizona, Tucson, AZ 85721-0207, United States.

Table of Contents

General Information	S2
Part I: Probe Design	S3-S6
Part II: Probe Synthesis and Structural Characterizations	S7-S8
Part III: Additional Fluorescence and Absorption Studies	S9-S12
Part IV: HRMS and ^{1}HNMR Studies of Reaction Products	S13-S14
Part V: Theoretical Calculations	S15-S16
Part VI: Detection of FA in Live Cells	S17-S20
Part VII: NMR and HRMS Data	S21-S23
References	S24

General Information

Commercial reagents were purchased from commercial suppliers and used as received, unless otherwise stated.

^{1}H and ^{13}C NMR spectra were recorded on Bruke DRX 400 (400 MHz). Mass Spectra were obtained from East China University of Science and Technology LC-Mass spectral facility. UV-Vis spectra were collected on a Shimadzu UV-1800 spectrophotometer. Fluorescence spectra were collected on a FluoroMax-4 (Horiba Scientific) fluorescence spectrophotometer with slit widths were set at 3 nm both for excitation and emission unless otherwise stated. The pH measurements were carried out with a FE20 plus (Mettler Toledo) pH meter.

Part I: Probe Design

1.1 Representative fluorescent probes for FA based on 2-aza-cope rearrangement

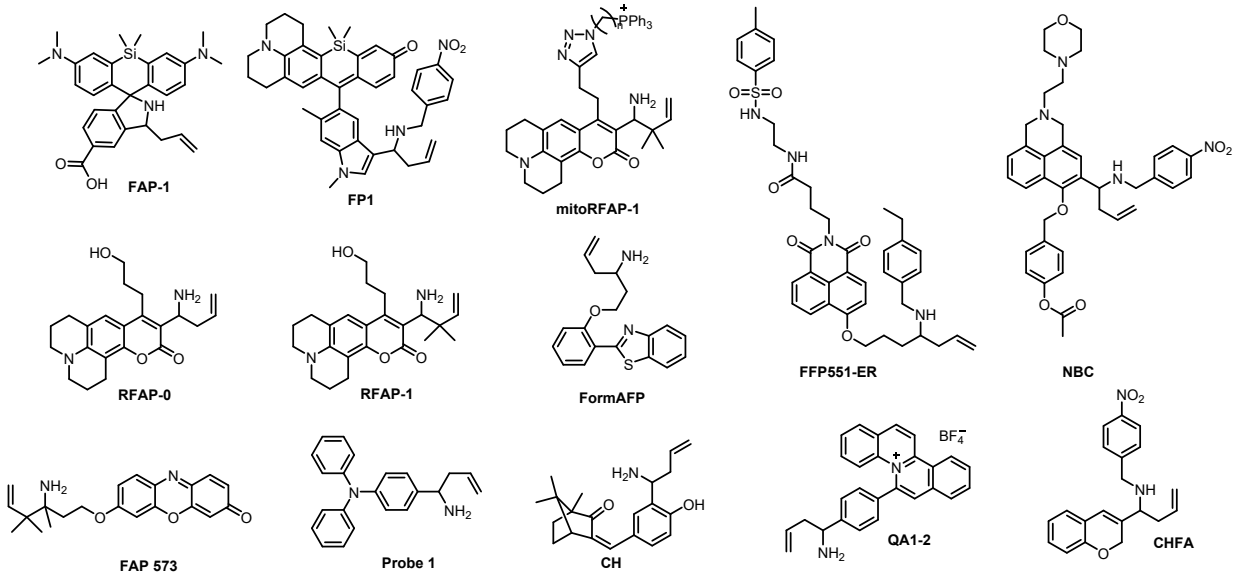

Figure S1 2-aza-cope rearrangement based fluorescent probes for FA.

1.2 Representative fluorescent probes for FA based on methylenehydrazine or formimine formation

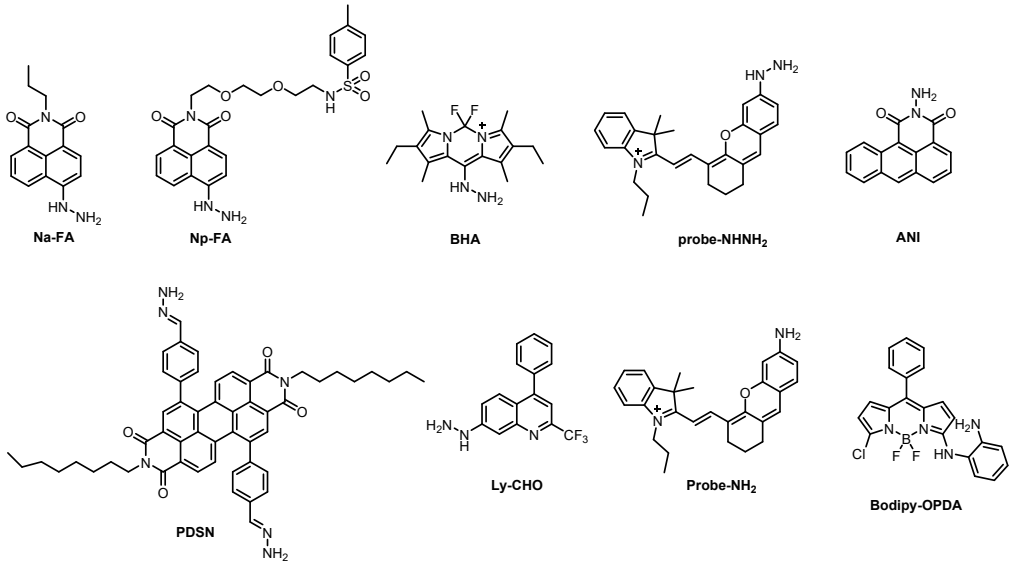

Figure S2 Methylenehydrazine or formimine formation based fluorescent probes for FA.

1.3 Representative fluorescent probes for FA based on diamine condensation/cyclization

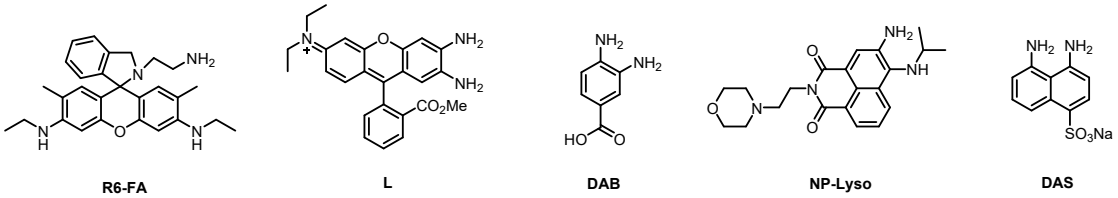

Figure S3 Diamine condensation/cyclization based fluorescent probes for FA.

1.4 Representative fluorescent probes for FA based on FA-induced intramolecularity

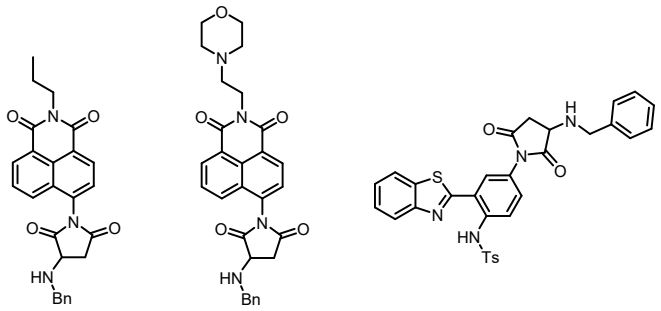

Figure S4 FA-induced intramolecularity based fluorescent probes for FA.

Table S1 Comparison of literature reported fluorescent probes for FA.
(N. A. means the information "not available" from the literature)

Probe	Ex nm	Em nm	LOD for FA μM	Optimized condition for FA detection	Biological application	Ref.
FAP-1	645	662↑ (turn-on)	5	10 μM probe +100 μM FA 2 h at 37 °C in PBS (20 mM, pH = 7.4)	HEK293T cells.	[1]
FP1	633	649↑ (turn-on)	10	1 μM probe + 250 μM FA 3 h at 37 °C in PBS (pH = 7.4)	HEK293TN cells NS1 cells	[2]
RFP-0 RFP-1	420/470	510↑ (turn-on)	0.3	10 μM probe +100 μM FA 2 h at 37 °C in PBS (20 mM, pH = 7.4)	HEK293T, HeLa, MCF-7, MCF-10A, RKO, SH-SY5Y and U-2OS cells	[3]
FAP-573	573	585↑ (turn-on)	N.A.	10 μM probe +100 μM FA 2 h at 37 °C in PBS (20 mM, pH = 7.4)	HEK293T, ADH5 KO, WT, HAP1 cells	[4]
FormAFP	340	520↑ (turn-on)	66 nM	20 μM probe + 500 μM FA 70 min at 37 °C in EtOH/PBS (1 : 50 v/v, 10 mM, pH = 7.4)	MCF7 cells	[5]
MitoRFAP-1	470	510↑ (turn-on)	N.A.	10 μM probe + 100 μM FA 120 min at 37 °C in PBS (10 mM, pH = 7.4)	HEK293T cells HeLa cells HCT-116 cells MCF-7 cells	[6]

FFP551-ER	441	551↑ (turn-on)	N.A.	10 μM + 100 μM FA 120 min at 37 °C in PBS (10 mM, pH = 7.4)	HeLa cells	[7]
NBC	485	525↑ (turn-on)	0.27	1 μM + 80 μM FA in PBS (100 mM, pH = 7.4)	HeLa cells mice	[8]
Probe 1	301	443↑ (turn-on)	14	10 μM probe + 1 mM FA 60 min in DMSO/ buffer solution (1 : 4 v/v, pH = 7.4)	Gaoliang Jiu sweet potato Jiu	[9]
CH	365	525↑ (turn-on)	2.01	20 μM probe + 1.4 mM FA in DMF/PBS buffer solution (1 : 19 v/v, 2 mM pH = 7.4)	Zebrafishs vermicelli chicken feet shrimp Xuanwu Lake	[10]
QA1-2	410	481↑ (turn-on)	5	10 μM probe + 10 mM FA at 37 °C in CH_3CN/PBS buffer solution (1 : 9 v/v, pH = 7.4)	filter paper strips	[11]
CHFA	360	517↑ (turn-on)	1.71	20 μM probe + 20 μM FA 180 min in at 37 °C CH_3CN/ PBS buffer solution (1 : 9 v/v, pH = 7.4)	HeLa cells	[12]
Na-FA	440	543↑ (turn-on)	0.71	5 μM probe + 100 μM FA 30 min in PBS (10 mM, pH = 7.4)	HeLa cells liver slides	[13]
Np-FA	450	540↑ (turn-on)	N.A.	6 μM probe + 150 μM FA 45 min in PBS (10 mM, pH = 7.4)	HeLa cells Zebrafishs Mouse brain tissue slices	[14]
BHA	420	466↑ (turn-on)	0.18	10 μM probe + 100 μM FA 32 min in PBS (10 mM, pH = 7.4)	HeLa cells	[15]
Probe-$NHNH_2$	670	706↑ (turn-on)	0.68	10 μM probe + 200 μM FA 10 min at 37 °C in PBS (10 mM, pH = 7.4)	HepG2 cells Zebrafish	[16]
ANI	440	518↑ (turn-on)	0.98	10 μM probe + 13 mM FA 3 min in DMF/PBS buffer solution (4 : 6 v/v, pH = 7.4)	HeLa cells	[17]
PDSN	450	625↑ (turn-on)	11.9 nM	20 μM probe + 2 mM FA in DMF/PBS buffer solution (1 : 1, v/v, pH = 7.4)	Food samples	[18]

Ly-CHO	400	514↑ (turn-on)	17.2 nM	10 μM probe + 100 μM FA in PBS (10 mM, pH = 7.4)	4T1 cells mice	[19]
Probe-NH_2	670	708↓ (turn-off)	1.87	10 μM probe +500 μM FA in PBS (10 mM, pH = 7.4)	filter paper strips mice	[20]
Bodipy-OPDA	482	548↑ (turn-on)	0.104	10 μM probe + 1000 μM FA 2 h at 37 °C in MeCN/HEPES (1:9, v/v, 20 mM, pH = 7.4)	filter paper strips HeLa cells	[21]
R6-FA	530	560↑ (turn-on)	0.77	10 μM probe +20 μM FA in DMF/PBS buffer solution (1 : 1, v/v, 25 mM, pH = 7.4)	filter paper strips HeLa cells	[22]
L	520	642↑ (turn-on)	8.3	5 μM probe +10 mM FA in EtOH/Tris-HCl (3 : 7, v/v, 10 mM, pH = 7.4)	L929 cells	[23]
DAB	344	430↑ (turn-on)	79 nM	10 μM probe + 800 μM FA 15 min in PBS (10 mM, pH = 7.4)	HepG2 cells HeLa cells WI-38 cells	[24]
NP-Lyso	380	444↑ (turn-on)	0.27	10 μM probe + 2 mM FA 60 min in PBS (10 mM, pH = 5.4)	L929 cells HeLa cells	[25]
DAS	345	490↑ (turn-on)	1	5 μM probe + 800 μM FA 60 min in PBS (10 mM, pH = 7.4)	HepG2 cells	[26]
NAP-FAP-1	359	470↑ (turn-on)	0.48	1 μM probe + 200 μM FA 15 min in PBS (10 mM, pH = 7.4)	HeLa cells THP-1 cells	[27]
NAP-FAP-2	359	472↑ (turn-on)	0.145	1 μM probe + 500 μM FA 30 min in PBS (10 mM, pH = 7.4)	HeLa cells THP-1 cells	[27]
ABTB	439	525↓440↑ (ratiometric)	0.43	10 μM probe +200 μM FA in aqueous solution	HeLa cells	[28]

Part II: Probe Synthesis and Structure Characterizations

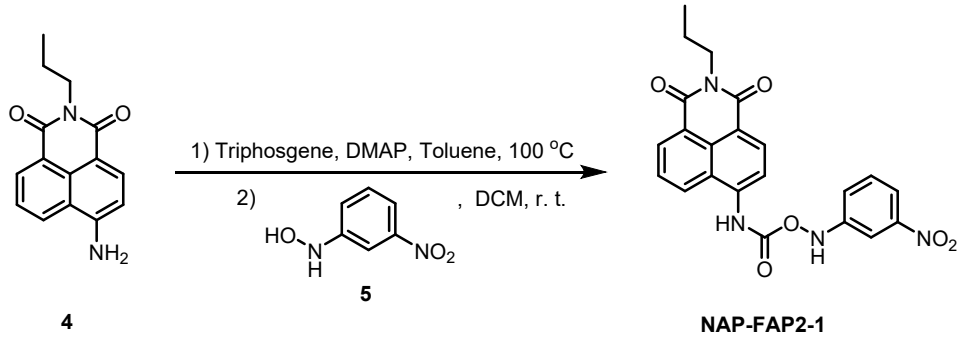

Scheme S1 Synthesis of the probe **NAP-FAP2-1**

2.1 3-nitrophenylazanyl *N*-(*N*-propyl-1,8-naphthalimide-4-yl)carbamate (NAP-FAP2-1)

To a solution of **4** [29] (25.4 mg, 0.100 mmol) and 4-dimethylaminopyridine (DMAP, 36.7 mg, 0.30 mmol) in 2 mL toluene under nitrogen atmosphere, was added triphosgene (45.5 mg, 0.15 mmol). The reaction mixture was heated to 100 °C and stirred at 100 °C for 6 h. After cooling to room temperature, a solution of *N*-(3-nitrophenyl) hydroxylamine (**5**)[30] (20 mg, 0.13 mmol) in 2 mL anhydrous dichloromethane was added to the reaction mixture. The reaction mixture was stirred at room temperature overnight. After the solvent was removed in vacuum by a rotavapor, the residue was purified by silica gel chromatography column using methylene chloride and methanol (20:1, v/v) as eluent to afford 21 mg (48 % yield) of the title probe **NAP-FAP2-1** as yellow solid. ^{1}H NMR (400 MHz, DMSO-d_6) δ 11.39 (s, 1H), 10.14 (s, 1H), 8.60 (t, J = 2.3 Hz, 1H), 8.57 - 8.48 (m, 3H), 8.14 (dd, J = 8.3, 2.3 Hz, 1H), 8.06 (d, J = 8.0 Hz, 1H), 7.96 (dd, J = 8.2, 2.3 Hz, 1H), 7.91 (t, J = 7.9 Hz, 1H), 7.68 (t, J = 8.3 Hz, 1H), 4.03 (t, J = 7.4 Hz, 2H), 1.67 (h, J =7.4 Hz, 2H), 0.94 (t, J = 7.4 Hz, 3H). ^{13}C NMR (150 MHz, DMSO-d_6): δ 163.4, 162.9, 153.8, 147.7, 143.3, 140.1, 131.1, 130.9, 129.8, 128.2, 126.4, 126.0, 125.9, 124.3, 122.2, 122.0, 118.4, 117.6, 112.6, 41.1, 20.8, 11.3. ESI-HRMS: m/z [M+Na]$^+$ calcd for [$C_{22}H_{18}N_4O_6Na$]$^+$: 457.1119, found: 457.1122.

2.2 3-nitrophenylazanyl *N*-(2-(4-methylbenzene-1-sulfonylamino)ethyl)-1,8-naphthalimide-4-yl)carbamate (NAP-FAP2-2)

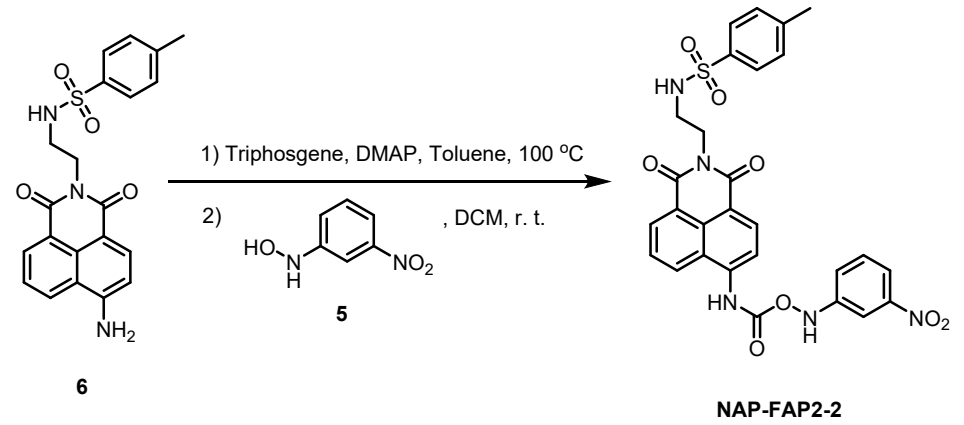

Scheme S2 Synthesis of the probe **NAP-FAP2-2**

To a solution of **6**[31] (20.5 mg, 0.050 mmol) and 4-dimethylaminopyridine (DMAP, 18.4 mg, 0.15 mmol) in toluene (2 mL) under nitrogen atmosphere and triphosgene (22.8 mg, 0.075 mmol) was added. The reaction mixture was stirred at 100 °C for 6 h. then the solution of *N*-(3-nitrophenyl) hydroxylamine[30] (10 mg, 0.065 mmol) in 2 mL anhydrous dichloromethane was added to the reaction mixture. The reaction mixture was stirred at room temperature overnight. After the solvent was removed in vacuum by a rotavapor, the residue was purified by silica gel chromatography column using methylene chloride and methanol (20:1, v/v) as eluent to afford 8.0 mg (27 % yield) of the probe **NAP-FAP2-2** as yellow solid. ^{1}H NMR (400 MHz, DMSO-d_6): δ 8.59 (t, J = 2.3 Hz, 1H), 8.51 - 8.40 (m, 3H), 8.14 (dd, J = 8.3, 2.2 Hz, 1H), 8.06 (d, J = 8.1 Hz, 1H), 7.93 (dd, J = 8.1, 2.3 Hz, 1H), 7.86 (t, J = 7.9 Hz, 1H), 7.75 (t, J = 6.4 Hz, 1H), 7.65 (t, J = 8.3 Hz, 1H), 7.59 (d, J = 8.1 Hz, 2H), 7.24 (d, J = 8.1 Hz, 2H), 4.12 (t, J = 6.6 Hz, 2H), 3.16-3.03 (m, 2H), 2.27 (s, 3H). ^{13}C NMR (125 MHz, DMSO-d_6) δ 163.6, 163.1, 153.9, 147.8, 143.4, 142.5, 140.1, 137.6, 131.1, 130.8, 129.9, 129.9, 129.5(2C), 128.4, 126.5 126.4(2C), 126.0, 124.4, 122.4, 122.0, 118.6, 117.7, 112.7, 40.1, 40.0, 20.9; ESI-HRMS: m/z $[M+Na]^+$ calcd for $[C_{28}H_{23}N_5O_8SNa]^+$: 612.1160, found: 612.1163.

Part III: Additional Fluorescence and Absorption Studies

All aqueous solutions were prepared using double distilled water. **NAP-FAP2-1** and **NAP-FAP2-2** stock solution (10 mM in dry DMSO) was prepared and stored at -20 °C. All fluorescence and absorption spectroscopic measurements were performed in 10 mM PBS buffer (pH 7.4) at 37 °C unless otherwise stated. Samples for absorption and fluorescence measurements were contained in 1 cm×1 cm quartz cuvettes (3.5 mL volume).

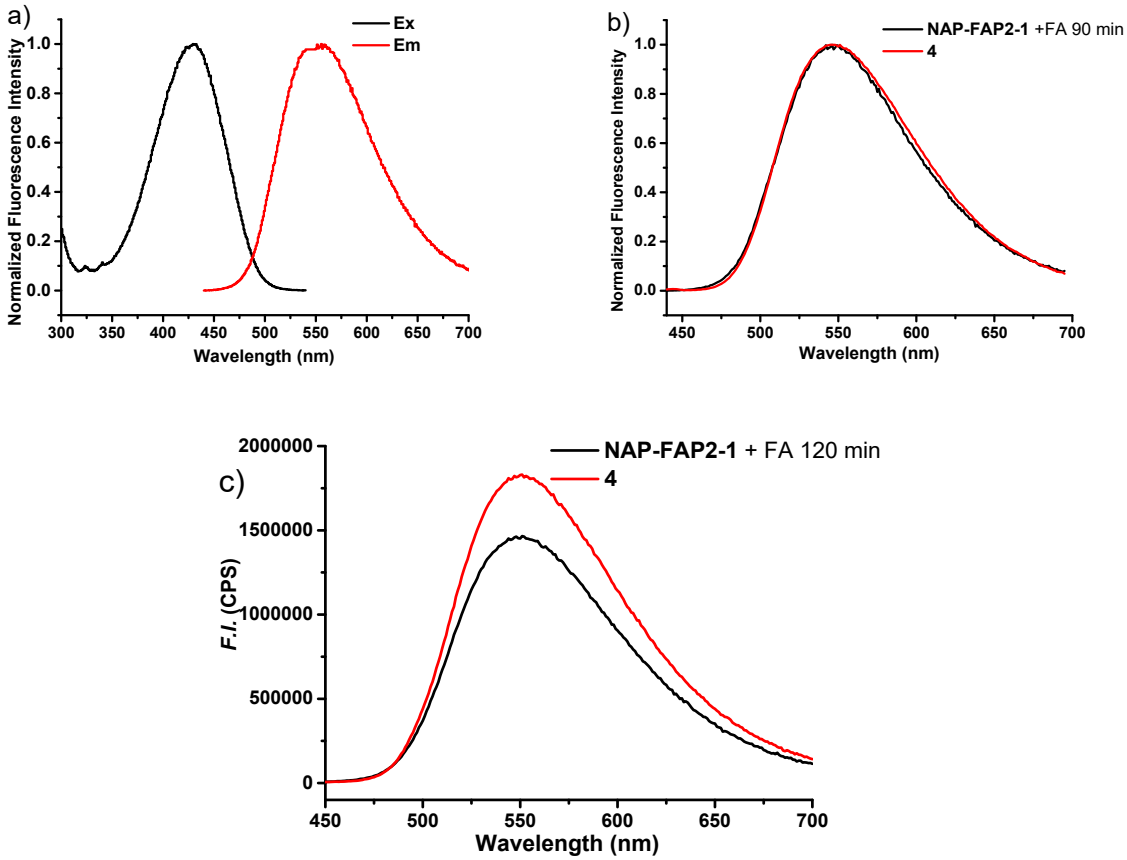

Figure S5 a) Normalized fluorescence excitation (λ_{em} = 550 nm) and emission spectra (λ_{ex} = 430 nm) of the probe **NAP-FAP2-1** (1 μM) upon incubation with 50 μM FA for 90 min; b) Overlap of the normalized fluorescence emission spectrum of the **NAP-FAP2-1** (1 μM) upon incubation with 50 μM FA for 90 min and that of the 4-amino-1,8-naphathalimide **4** (1 μM, λ_{ex} = 430 nm); c) Comparison of fluorescence emission spectrum of the reaction mixture of **NAP-FAP2-1** (1 μM) upon incubation with 50 μM FA for 120 min with that of the fluorescent product **4** (1 μM, λ_{ex} = 430 nm).

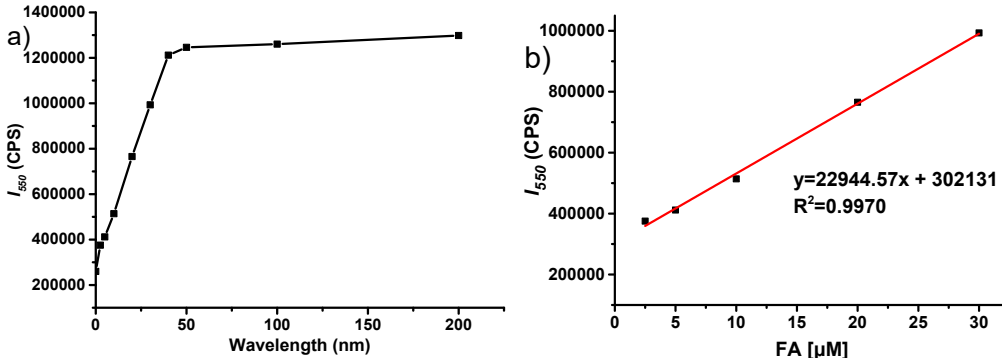

Figure S6 a) Fluorescence intensity of the probe **NAP-FAP2-1** (1 μM) at 550 nm (λ_{ex}=430 nm) after incubation with FA for 90 min versus [FA]. The maximum fluorescence intensity at 550 nm was achieved with addition of 50 μM FA; b) Linear regression of the fluorescence intensity at 550 nm (λ_{ex}=430 nm) versus FA concentrations (2.5 to 30 μM): the limit of detection (LOD, S/N=3 and N=6748 CPS) = 0.88 μM.

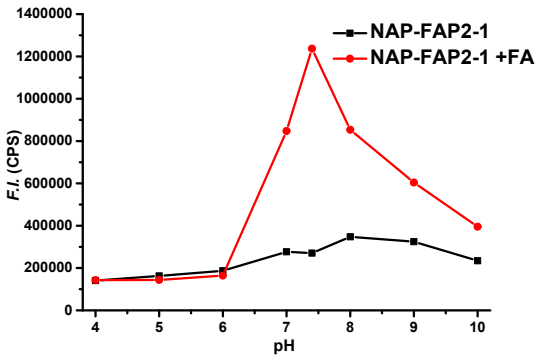

Figure S7 pH-dependent fluorescence intensity at 550 nm (λ_{ex}=430 nm) of the probe **NAP-FAP2-1** (1 μM) incubated with 50 μM FA for 90 min.

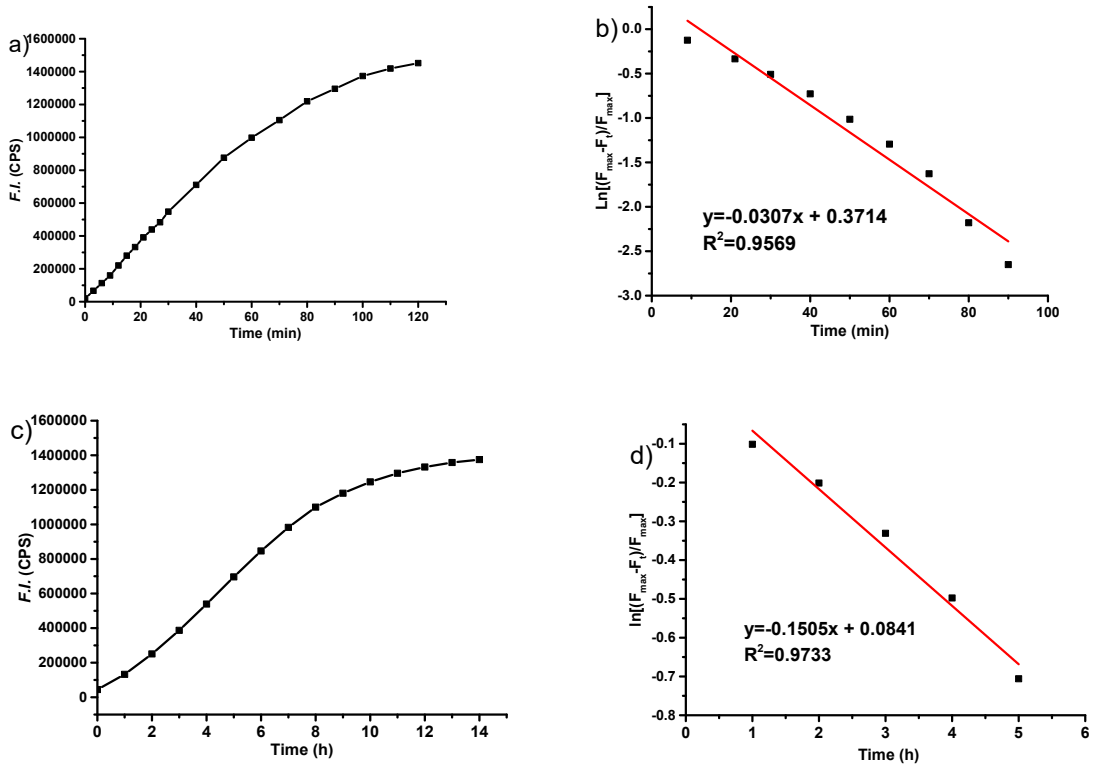

Figure S8 a) Time-dependent (0 – 120 min) fluorescence intensity of the **NAP-FAP2-1** (1 μM) upon incubation with 50 μM FA at 550 nm (λ_{ex}=430 nm) and b) the corresponding linear regression of $Ln[(F_{max}-F_t)/F_{max}]$ versus incubation time (10 - 90 min). The calculated pseudo first-order reaction kinetic constant was 0.0307 min^{-1}, and the second-order reaction kinetic constant was 10.2 $M^{-1}s^{-1}$; c) Time-dependent (0 - 14 h) fluorescence intensity of the **NAP-FAP2-1** (1 μM) self-hydrolysis at 550 nm (λ_{ex}=430 nm) and d corresponding linear regression of $Ln[(F_{max}-F_t)/F_{max}]$ versus t (1-5 h). The calculated pseudo first-order reaction kinetic constant was 0.1505 h^{-1} (0.0025 min^{-1}), and the second-order reaction kinetic constant was 7.5×10^{-7} $M^{-1}s^{-1}$.

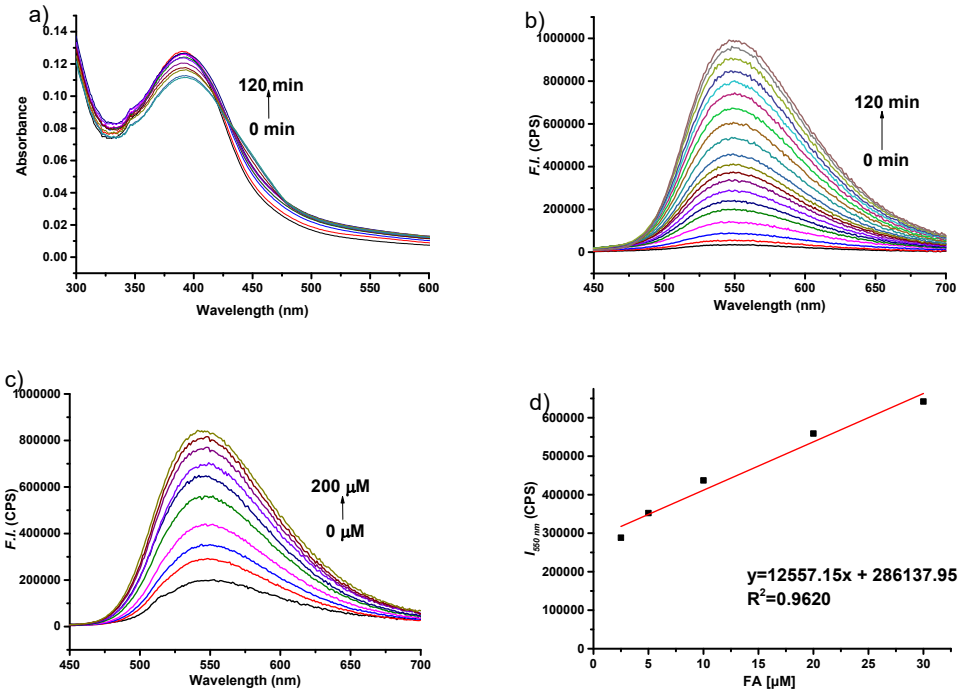

Figure S9 a) Time-dependent absorption spectra of the probe **NAP-FAP2-2** (10 μM) upon addition of 500 μM FA; b) Time-dependent fluorescence emission spectra (λ_{ex}=438 nm) of the probe **NAP-FAP2-2** (1 μM) upon addition of 50 μM FA with 28.1 fold of fluorescence intensity increase at 550 nm; c) Concentration-dependent fluorescence emission spectra (λ_{ex}=438 nm) of the **NAP-FAP2-2** (1 μM) upon addition of increasing amount of FA (0-200 μM); d) Linear regression of the fluorescence intensity at 550 nm (λ_{ex}=438 nm) versus FA concentrations (2.5 to 30 μM): the limit of detection (LOD, S/N=3 and N=3892 CPS) = 0.93 μM.

Part IV: HRMS and ^{1}HNMR Studies of Reaction Products

4.1 HRMS studies of reaction mixture of the probe NAP-FAP2-1 with FA.

To a suspended solution of the probe **NAP-FAP2-1** (4.3 mg, 0.010 mmol) in 1 mL THF was added 10 equiv. FA (40% FA in H_2O, 7.5 μL). The mixture was stirred at 37 ℃ for 8 h. The reaction solution was extracted with ethyl acetate. The organic phase was separated, dried in vaccuo, then taken for HRMS analysis. The peak m/z 255.1135 was assigned to the $[M+H]^+$ peak of the 4-amino-1,8-naphthalimide **4** with the calculated value m/z as 255.1134 (**Scheme S3**).

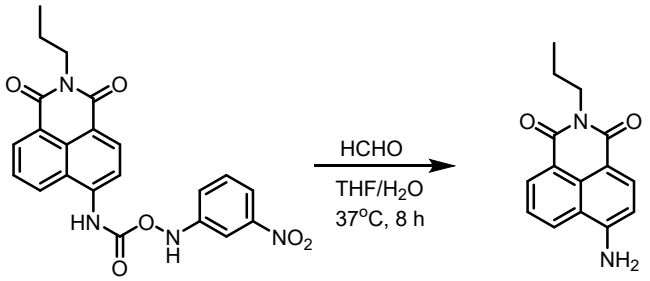

Scheme 3 Scale-up reaction of the probe **NAP-FAP2-1** and FA in THF and water.

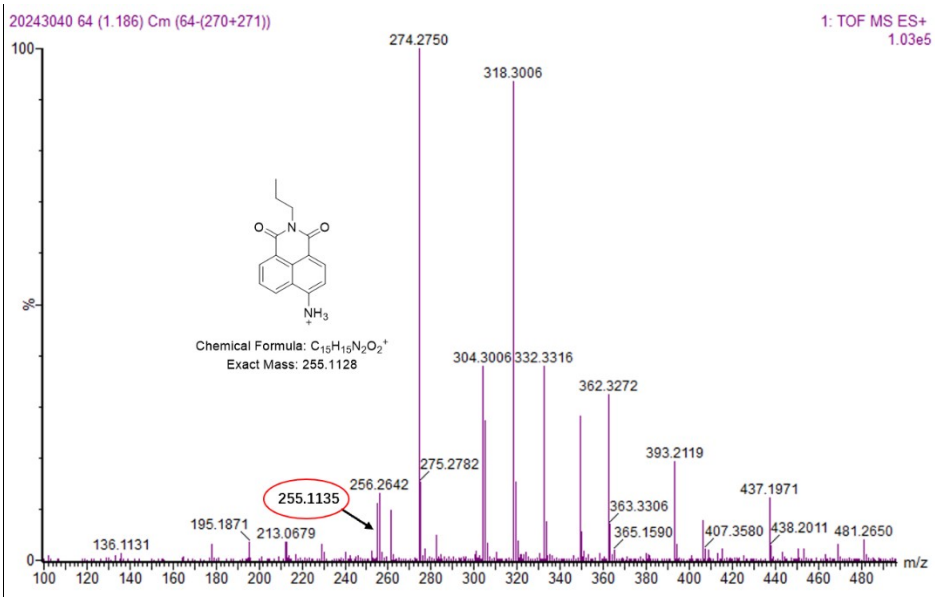

Monoisotopic Mass, Even Electron Ions

3336 formula(e) evaluated with 9 results within limits (all results (up to 1000) for each mass)

Elements Used:

12C: 0-60 13C: 0-1 H: 0-60 N: 1-6 O: 1-6 Na: 0-1

Minimum:	10.00					-1.5
Maximum:	100.00		20.0	10.0		50.0
Mass	RA	Calc. Mass	mDa	PPM		DBE
i-FIT	Norm	Conf(%)	Formula			
255.1135	100.00	255.1134	0.1	0.4	9.5	135.9	0.256
77.42		12C15 H15 N2 O2				

Figure S10 ESI-HRMS spectrum of the reaction mixture of **NAP-FAP2-1** and FA.

4.2 ^{1}HNMR studies of reaction mixture of the probe NAP-FAP2-1 with FA

To a suspended solution of the probe **NAP-FAP2-1** (6.5 mg, 0.015 mmol) in 1.5 mL THF was added 10 equiv. FA (40% FA in H_2O, 11.3 μL). The mixture was stirred at 37 ℃ for 8 h. The reaction solution was extracted with ethyl acetate. The organic phase was separated, dried in vaccuo, the residue was purified by silica gel chromatography column using methylene chloride and methanol (20:1, v/v), then taken for ^{1}HNMR analysis.

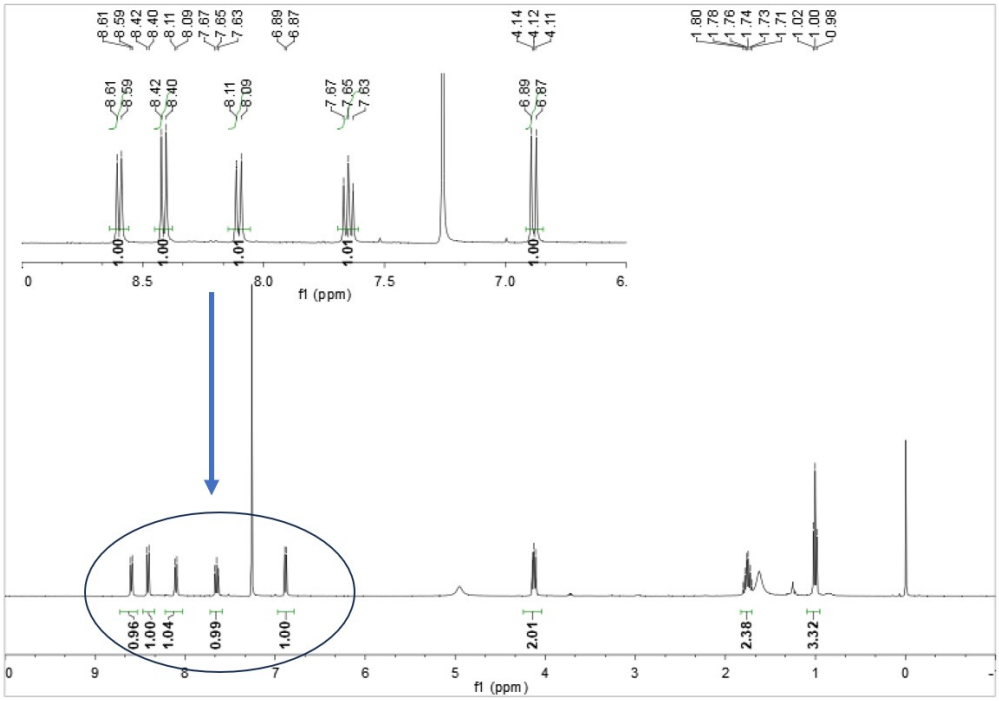

Figure S11 ^{1}HNMR spectrum of the 4-amino-1,8-naphthalimide.

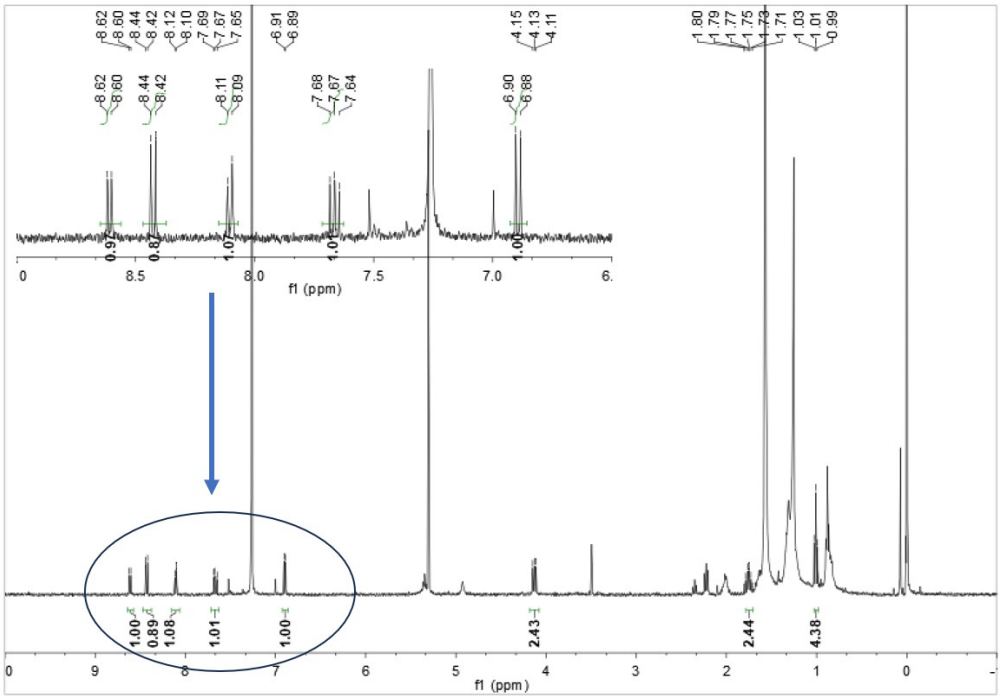

Figure S12 ^{1}HNMR spectrum of the product from reaction mixture of **NAP-FAP2-1** and FA..

Part V Theoretical Calculations

All theoretical calculations [density functional theory (DFT) and the time-dependent DFT (TDDFT)] were carried out using Gaussian 09 software.[32] The ground state structures of the simplified probe structure **NAP-FAP2-Me** (Figure S8), was optimized using DFT with B3LYP functional and 6-31G (d, p) basis set (considered as in gas phase). The excited state related calculations were carried out with the TDDFT, based on the optimized structure of the ground state. There are no imaginary frequencies in all calculated structures during the frequency analysis.

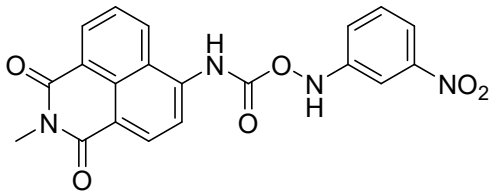

NAP-FAP2-Me

Figure S13 Structure of **NAP-FAP2-Me**

Table S2 Atomic coordinates of the ground state structure optimized from DFT B3LYP/6-31G (d,p).

Atom#	Atom Type	x	y	z
1	C	4.664226	-2.39309	-0.20907
2	C	3.448762	-3.05702	0.043518
3	C	2.292477	-2.33702	0.278222
4	C	2.290921	-0.9164	0.26788
5	C	3.533492	-0.24775	0.027223
6	C	4.706778	-1.01025	-0.21279
7	C	1.121857	-0.10826	0.491513
8	C	1.217501	1.276811	0.501195
9	C	2.454704	1.904353	0.276816
10	C	3.601141	1.168886	0.034767
11	N	-0.10408	-0.77271	0.679179
12	C	-1.29643	-0.24302	1.084714
13	O	-1.55605	0.906956	1.373696
14	O	-2.21475	-1.27479	1.163886
15	N	-3.52117	-0.8411	1.553133
16	C	-4.39526	-0.7191	0.442686
17	C	-5.44313	0.204516	0.529056
18	C	-6.37501	0.251119	-0.50342
19	C	-6.30145	-0.57228	-1.62582
20	C	-5.24507	-1.48026	-1.69534
21	C	-4.30034	-1.5662	-0.67099
22	C	4.880837	1.873706	-0.21123
23	N	6.008688	1.068936	-0.45343

24	C	6.003422	-0.32861	-0.46868
25	O	7.039055	-0.94792	-0.68633
26	O	4.967536	3.096105	-0.20826
27	C	7.301078	1.721056	-0.70698
28	N	-7.47863	1.227771	-0.40361
29	O	-8.28818	1.272064	-1.33
30	O	-7.52575	1.939964	0.600275
31	H	5.579387	-2.94448	-0.39575
32	H	3.420791	-4.14176	0.060803
33	H	1.386226	-2.89658	0.489981
34	H	0.334446	1.873669	0.680526
35	H	2.522069	2.986924	0.281978
36	H	-0.1291	-1.76663	0.505449
37	H	-3.38925	0.054049	2.027465
38	H	-5.5452	0.877304	1.372676
39	H	-7.04705	-0.49488	-2.40627
40	H	-5.15931	-2.13677	-2.55526
41	H	-3.49185	-2.28501	-0.72927
42	H	7.686023	1.406485	-1.67912
43	H	7.140962	2.796071	-0.68593
44	H	8.020328	1.425081	0.059916

Table S3 Overview of theoretical calculations of main electron transitions based on TDDFT//B3LYP/6-31G(d,p) calculation on the optimized ground structure of **NAP-FAP2-Me**

Electronic Transition	TDDFT//B3LYP/6-31G(d,p)			
	Energy (eV)	*f*	Main Configuration	CI coefficients
$S_0 \rightarrow S_1$	3.38 eV, 367 nm	0.2351	HOMO→LUMO+1	0.6573
$S_0 \rightarrow S_2$	3.39 eV, 366 nm	0.0909	HOMO→LUMO	0.6254
$S_0 \rightarrow S_3$	3.53 eV, 352 nm	0.0159	HOMO-1→LUMO	0.6079

Part VI: Detection of FA in Live Cells

Cell culture: The murine macrophage RAW264.7 cell lines were kindly provided by Stem Cell Bank, Chinese Academy of Sciences. RAW264.7 cells were cultured in DMEM media (Adamas) supplied with 10% Fetal Bovine Serum (FBS, Sangon Biotech), 1% Penicillin-Streptomycin (Gibco) at 37 °C in a humidified atmosphere containing 95% air and 5% CO_2.

6.1 Cytotoxicity assay of the NAP-FAP2-1 and NAP-FAP2-2 for RAW264.7 cells

Cell growth assay was performed using Cell Counting Kit-8 (Elabscience Biotechnology). Cell were seeded in 96-well plates with an initial seeding density of 10000 cells per well. Solutions of **NAP-FAP2-1** and **NAP-FAP2-2** (0, 5, 10, 20, 50 and 100 μM) were added into the wells and incubated for 8 h at 37°C. 2-(2-Methoxy-4-nitrophenyl)-3-(4-nitrophenyl)-5-(2,4-disulfobenzene)-2H-tetrazole monosodium salt (CCK8, 10 μL) was then added into each well for further incubation 1 h. Absorbance was read by a microplate reader (BioTek Synergy Lx) at wavelength λ=450 nm.

Cell Viability (% of control) = (Medicated cells OD / Control cells OD) * 100%

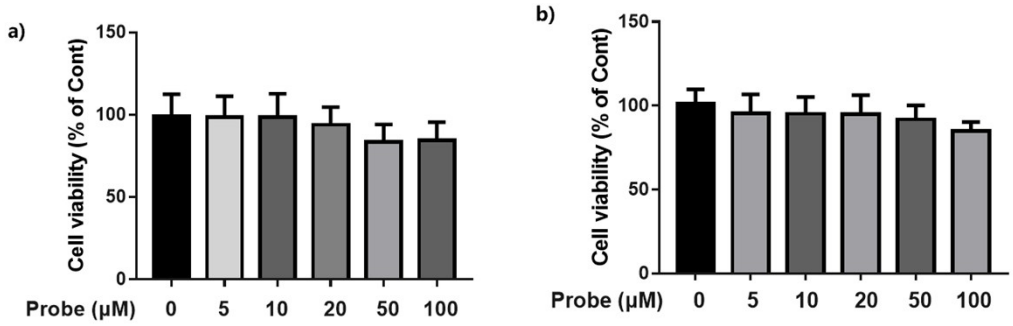

Figure S14 a) Cell viabilities of RAW264.7 cells incubated with **NAP-FAP2-1** at various concentrations for 8 h; b) Cell viabilities of RAW264.7 cells incubated with **NAP-FAP2-2** at various concentrations for 8 h.

6.2 Confocal fluorescence imaging studies of NAP-FAP2-1 for FA level changes in RAW264.7 cells due to exogenous FA incubation

RAW264.7 cells were seeded in a T-25 cell culture flask in DMEM medium with 10% Fetal Bovine Serum and 1% Penicillin-Streptomycin at 37 ˚C for 48 hours. One day before the experiment, RAW264.7 cells were transferred to Nunc 35 mm glass-bottom cell culture dishes (Thermo Scientific) to allow the cells to adhere. For imaging studies, three groups of cells were incubated without FA, 100 μM FA, and 200 μM FA, respectively for 1 h. Another group of cells were co-incubated with 200 μM FA and 300 μM $NaHSO_3$ for 1 h. Then, the cells were washed with HBSS and then incubated with 20 μM **NAP-FAP2-1** in culture medium for 90 min. After incubation, fresh culture medium was replaced, then cell fluorescence images were captured on a Leica TCS SP8 equipped with 63× objective lens and PMT gain of 800 ($\lambda_{ex/em}$ = 458/555±25 nm). The results were shown in **Figure 4**.

6.3 Confocal fluorescence imaging studies of NAP-FAP2-1 for FA level changes during erastin-induced ferroptosis in RAW264.7 cells

RAW264.7 cells were seeded in a T-25 cell culture flask in DMEM medium with 10% Fetal Bovine Serum and 1% Penicillin-Streptomycin at 37 ˚C for 48 hours. One day before the experiment,

RAW264.7 cells were transferred to Nunc 35 mm glass-bottom cell culture dishes (Thermo Scientific) to allow the cells to adhere. For imaging the ferroptosis process, RAW 264.7 cells were treated with 10 μM erastin in the presence or absence of 10 μM Fer-1 at 37 °C for the indicated times (0, 4 and 8 h). The cells were washed with HBSS and then incubated with 20 μM **NAP-FAP2-1** in culture medium for 90 min. After incubation, the cell medium were replaced with a new culture medium, then imaged on a Leica TCS SP8 equipped with 63× objective lens and PMT gain of 800 ($\lambda_{ex/em}$ = 458/555±25 nm). Results were shown in **Figure 5**.

6.4 Confocal fluorescence imaging studies of NAP-FAP2-2 and ER Red tracker in RAW 264.7 cells due to exogenous FA incubation

RAW 264.7 cells were seeded in a T-25 cell culture flask in DMEM medium with 10% Fetal Bovine Serum and 1% Penicillin-Streptomycin at 37 ˚C for 48 hours. One day before the experiment, cells were transferred to Nunc 35 mm glass-bottom cell culture dishes (Thermo Scientific) to allow the cells to adhere. For colocalization imaging studies, cells were incubated with FA (0, 100, and 200 μM) for 1 h. Another group co-incubated with 200 μM FA and 300 μM $NaHSO_3$ for 1 h. Then, the cells were washed with HBSS and then incubated with 20 μM **NAP-FAP2-2** in culture medium for 90 min, and then 200 nM ER Tracker Red was added and incubated for further 20 min, the cells were washed with HBSS and then imaged on a Leica TCS SP8 equipped with 40× objective lens and PMT gain of 800 ($\lambda_{ex/em}$ = 458/555±25 nm, $\lambda_{ex/em}$ = 561/610±15 nm). Pearson's colocalization coefficients were analyzed with Image J software. The results were shown in **Figure S15**.

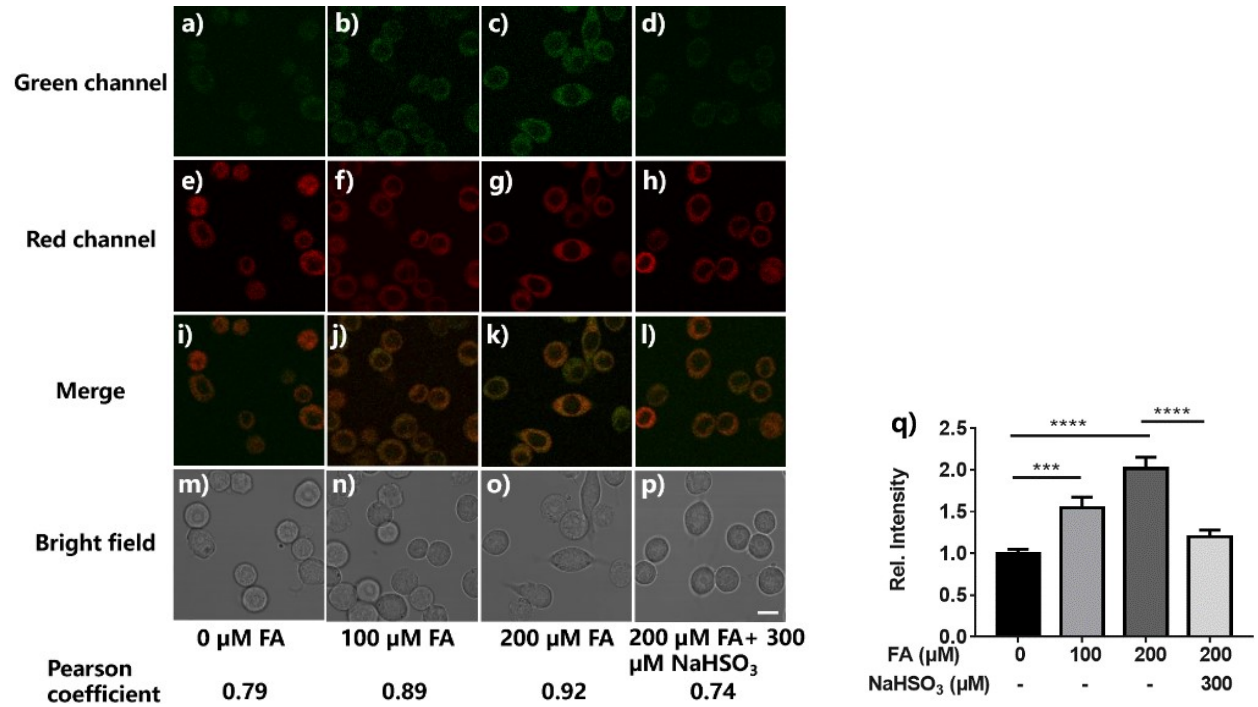

Figure S15 Colocalization fluorescence imaging studies of **NAP-FAP2-2** and ER Red for exogenous FA incubation in RAW 264.7 cells: a, e, i, m) Cells were incubated in normal media and then incubated in 20 μM **NAP-FAP2-2** for 90 min and then 200 nM ER Tracker Red for 20 min; b, f, j, n) Cells were incubated in 100 μM FA for 1 h, and then incubated in 20 μM **NAP-FAP2-2** for 90 min and then 200 nM ER Tracker Red for 20 min; c, g, k, o) Cells were incubated in 200 μM FA for 1 h, and then incubated in 20 μM **NAP-FAP2-2** for 90 min and then 200 nM ER Tracker Red for 20 min; d, h, l, p)

Cells were incubated in 200 μM FA and 300 μM $NaHSO_3$ for 1 h, and then incubated in 20 μM **NAP-FAP2-2** for 90 min and then 200 nM ER Tracker Red for 20 min; m-p) Corresponding bright-field images; q) Relative fluorescence intensities of RAW 264.7 cells in green channel of the fluorescence images in different cell groups. Cell images were captured on a Leica TCS with 63× objective lens and PMT gain of 800 ($\lambda_{ex/em}$ = 458/555±25 nm, $\lambda_{ex/em}$ = 561/610±15 nm), scale bar = 10 μm. (Error bars represent the standard deviations of three replicates; ****P ≤ 0.0001, ***P ≤ 0.001.)

Standard procedure for probe incubation and flow cytometry analysis: The cells were washed with HBSS and then incubated with 20 μM **NAP-FAP2-1** or **NAP-FAP2-2** in culture medium for 90 min. After incubation, the cells were washed with HBSS and then subjected to mild centrifugation at 350×g for 5 min. The supernatant was discarded, and cells was resuspended in 200 μL PBS and kept at 4 ˚C in dark for analysis with a flow cytometer (Beckman Instruments, USA, $\lambda_{ex/em}$ = 488/585 nm).

6.5 Flow cytometry studies of NAP-FAP2-1 for FA level changes in RAW 264.7 cells due to exogenous FA incubation

RAW264.7 cells were seeded in a T-25 cell culture flask in DMEM medium with 10% Fetal Bovine Serum and 1% Penicillin-Streptomycin at 37 ˚C for 48 hours. One day before the experiment, cells were transferred to a 35 mm tissue culture dishes (Thermo Scientific) to allow the cells to adhere. Cells were incubated with FA (0, 100, and 200 μM) for 1 h. Another group was co-incubated with 200 μM FA and 300 μM $NaHSO_3$ for 1 h, and then was subjected to the standard procedure shown above using the probe **NAP-FAP2-1** for further probe incubation and flow cytometry analysis. Results were shown in Figure **S16**.

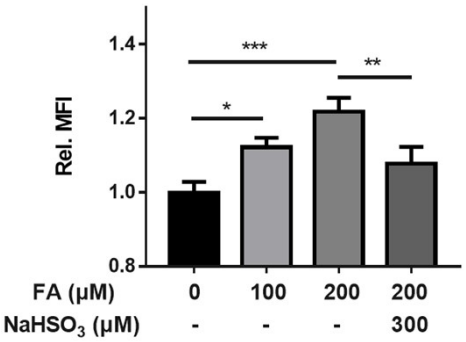

Figure S16 Flow cytometry analysis of relative fluorescence intensities of RAW 264.7 cells upon treatment with different concentrations of FA in the presence or absence of 300 μM $NaHSO_3$ for 1 h. (Error bars represent the standard deviations of three replicates, ***P ≤ 0.001, **P ≤ 0.01, *P ≤ 0.1).

6.6 Flow cytometry studies of FA level changes in cytoplasm and endoplasmic reticulum during erastin-induced ferroptosis in RAW264.7 cells

RAW264.7 cells were seeded in a T-25 cell culture flask in DMEM medium with 10% Fetal Bovine Serum and 1% Penicillin-Streptomycin at 37 ˚C for 48 hours. One day before the experiment, cells were transferred to a to a 35mm tissue culture dishes (Thermo Scientific) to allow the cells to adhere. For studying the ferroptosis process, RAW264.7 cells were treated with 10 μM erastin (diluted from 20 mM stock in DMSO with the cell culture media) in the presence or absence of 10 μM Fer-

1(diluted from 50 mM stock in DMSO with the cell culture media) at 37 °C for the indicated times (0, 4, and 8 h), and then proceed to flow cytometry analysis. And then applied the standard procedure using the probe **NAP-FAP2-1** and **NAP-FAP2-2** for probe incubation and cytometry analysis. The results were shown in **Figure 6**.

Part VIII: NMR and HRMS Data

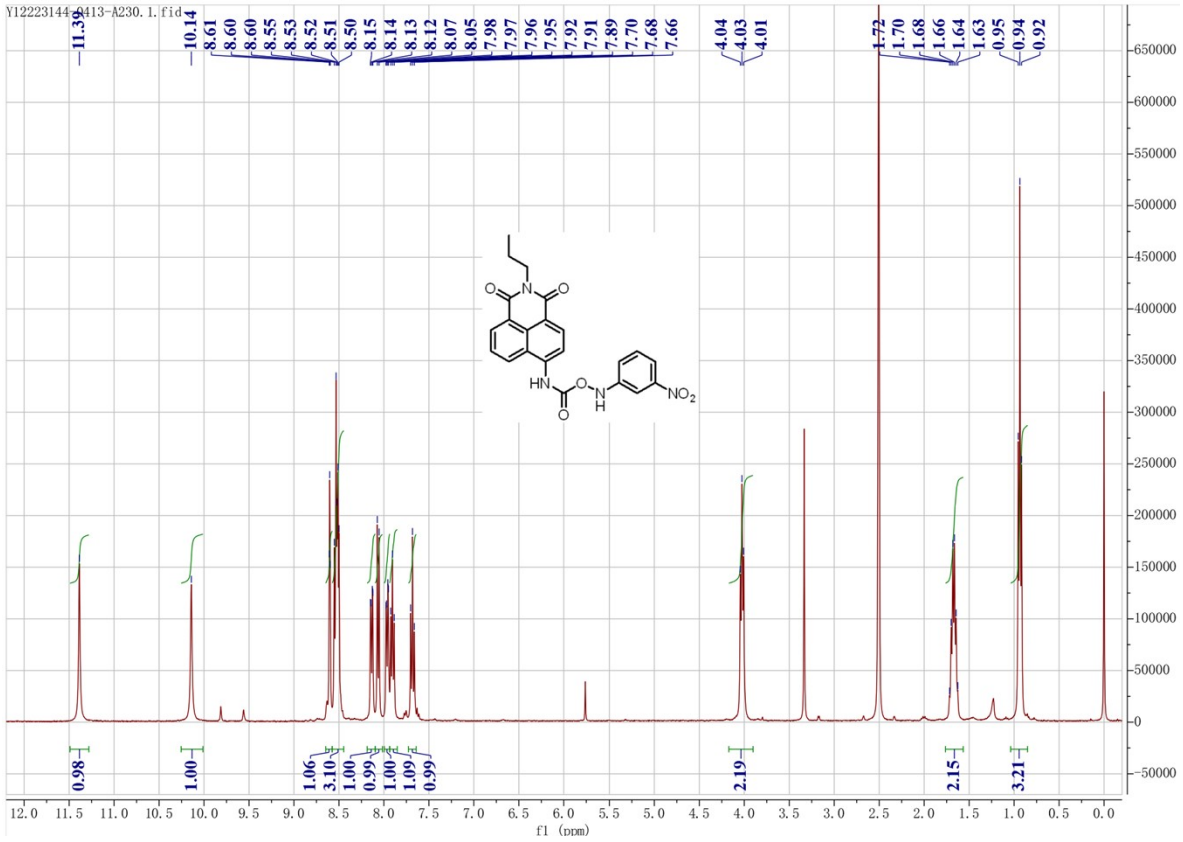

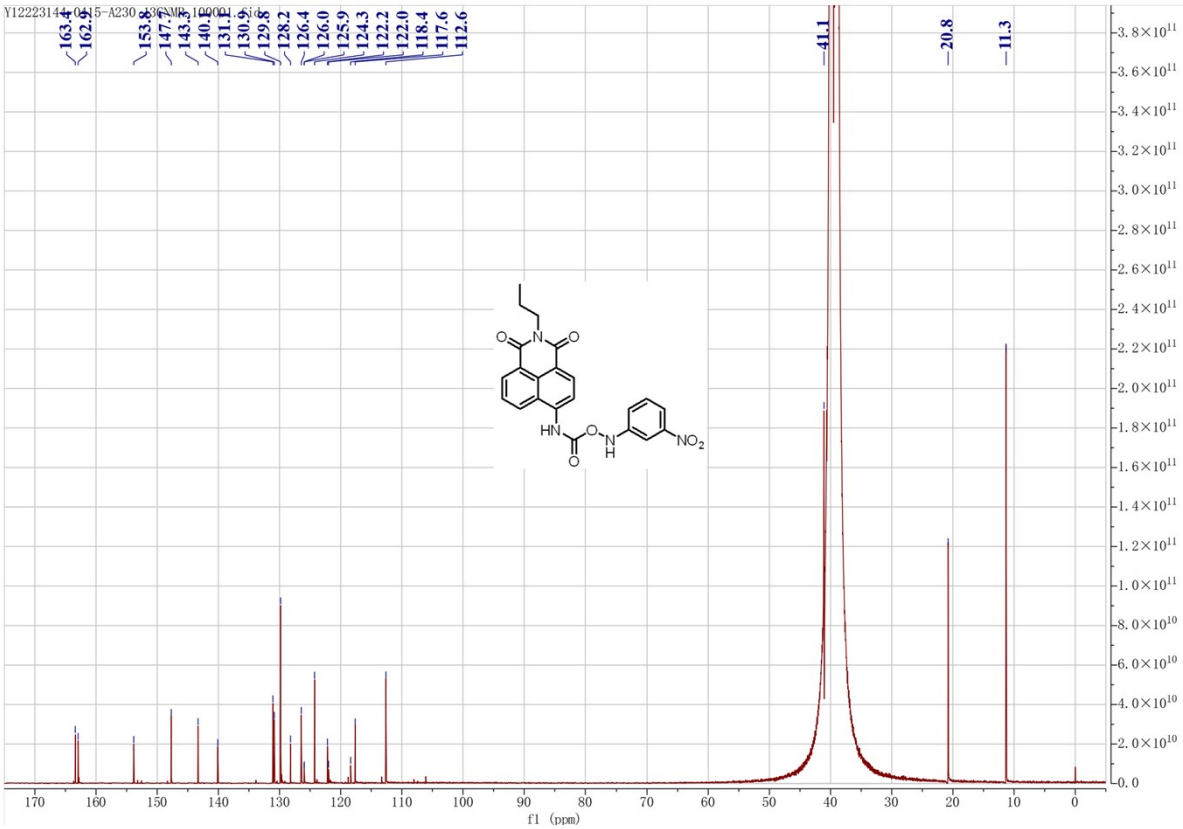

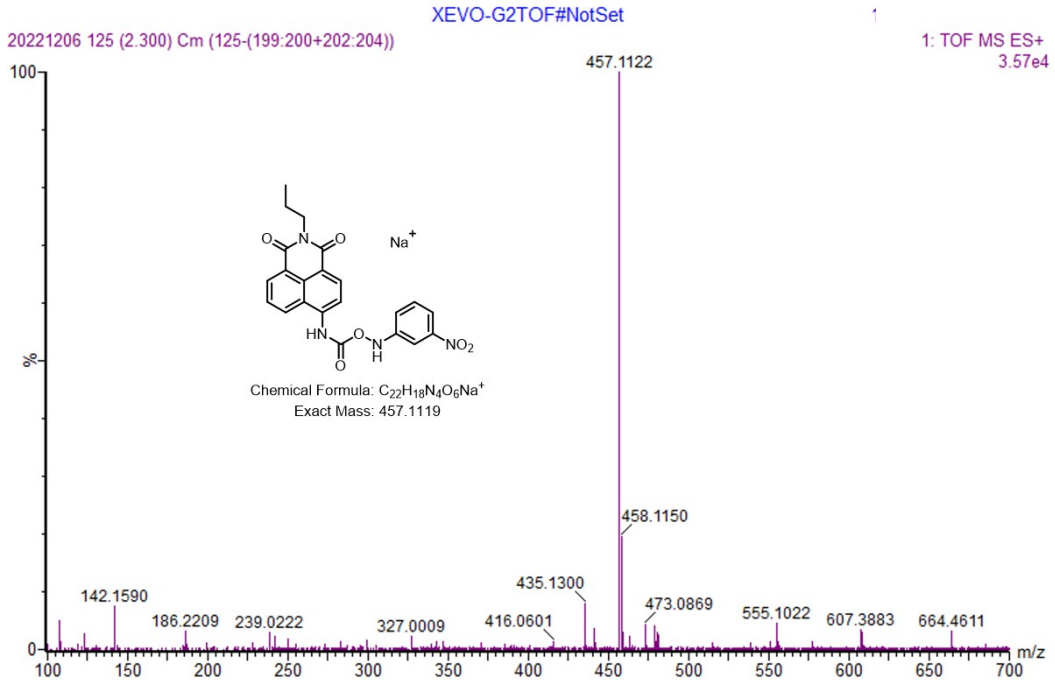

Figure S17 ^{1}H NMR, ^{13}C NMR, and HRMS of the probe **NAP-FAP2-1**

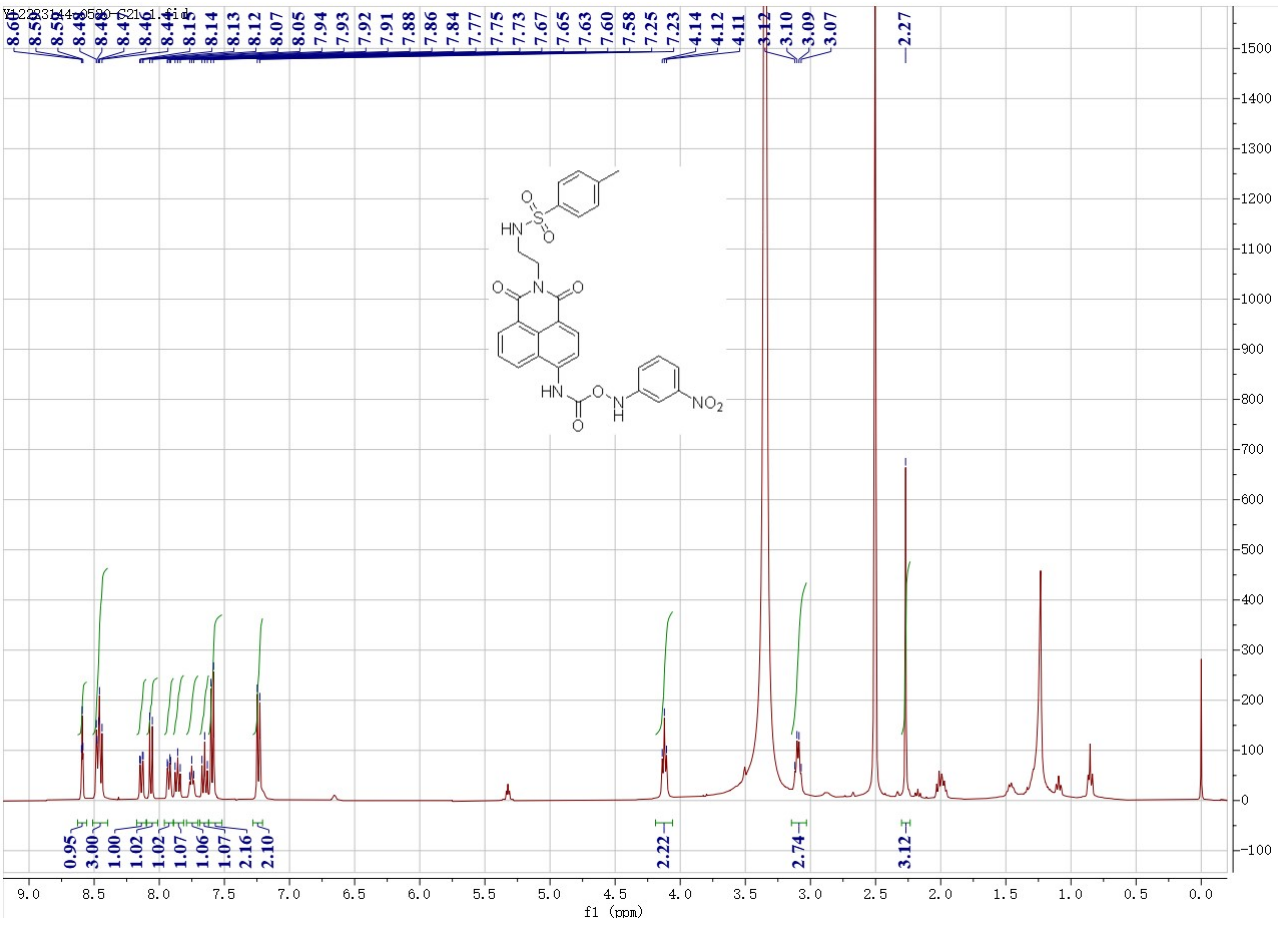

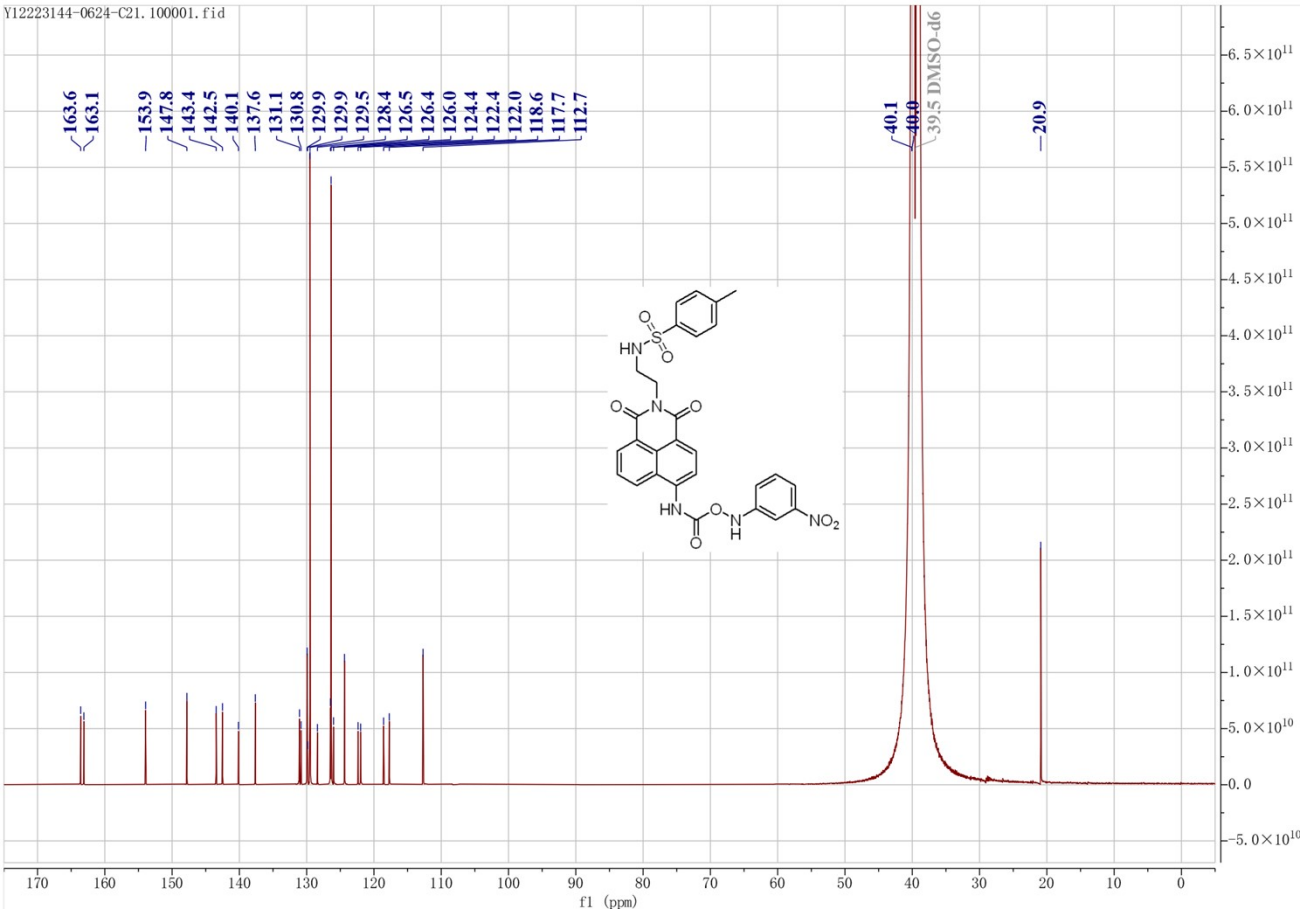

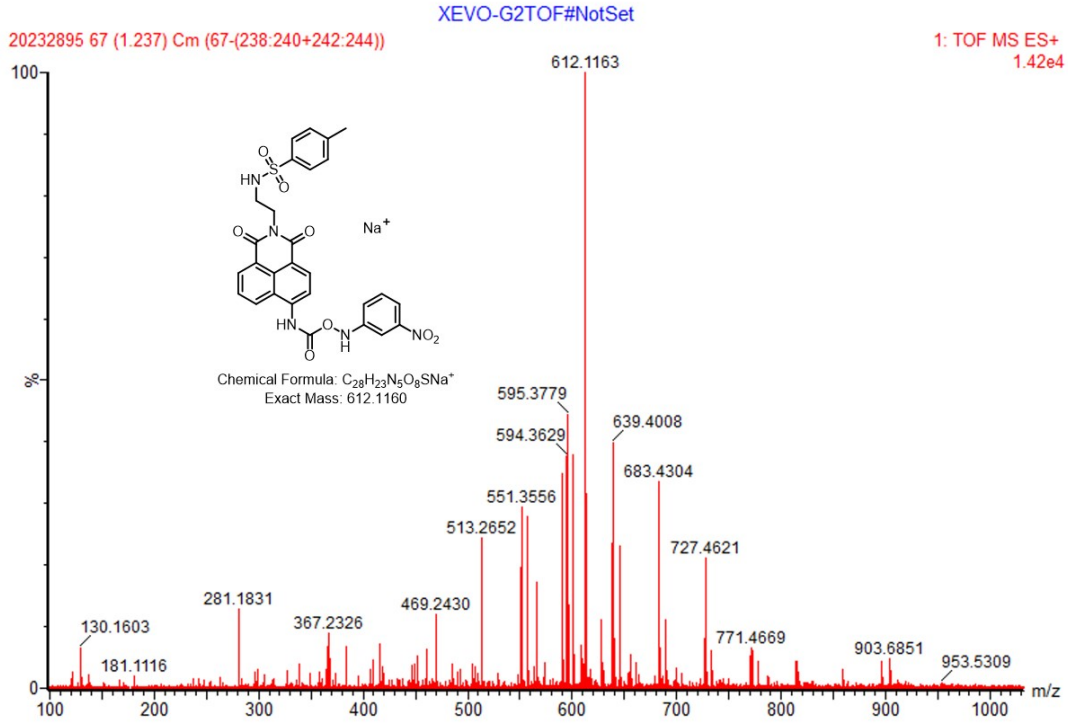

Figure S18 ^{1}H NMR, ^{13}C NMR, and HRMS of the probe **NAP-FAP2-2**.

References

1. Brewer, T. F.; Chang, C. J., *J. Am. Chem. Soc.* **2015,** *137* (34), 10886-10889.
2. Roth, A.; Li, H.; Anorma, C.; Chan, J., *J. Am. Chem. Soc.* **2015,** *137* (34), 10890-10893.
3. Brewer, T. F.; Burgos-Barragan, G.; Wit, N.; Patel, K. J.; Chang, C. J., *Chem. Sci.* **2017,** *8* (5), 4073-4081.
4. Bruemmer, K. J.; Walvoord, R. R.; Brewer, T. F.; Burgos-Barragan, G.; Wit, N.; Pontel, L. B.; Patel, K. J.; Chang, C. J., *J. Am. Chem. Soc.***2017,** *139* (15), 5338-5350.
5. Quan, T.; Liang, Z.; Pang, H.; Zeng, G.; Chen, T., *Analyst* **2022,** *147* (2), 252-261.
6. Tenney, L.; Pham, V. N.; Brewer, T. F.; Chang, C. J., *Chem. Sci.* **2024,** *15* (21), 8080-8088.
7. Zhang, Y.; Du, Y.; Liao, K.; Peng, T., *Anal. Methods* **2024,** *16* (23), 3646-3653.
8. Liu, J.; Li, K.; Xue, P.; Xu, J., *Anal. Biochem.* **2022,** *652*, 114749.
9. Deng, B.; Ding, L.; Yang, S.; Tian, H.; *Luminescence* **2023,** *38* (9), 1647-1653.
10. Liang, Y.; Zhang, Y.; Li, M.; Meng, Z.; Gong, S.; Du, W.; Yang, Y.; Wang, Z.; Wang, S., *Microchem. J.* **2022,** *177*, 107305.
11. Tantipanjaporn, A.; Ka-Yan Kung, K.; Sit, H.-Y.; Wong, M.-K., *RSC Adv.* **2022,** *12* (18), 11543-11547.
12. Wang, Y.; Chen, Y.; Huang, Y.; Zhang, Q.; Zhang, Y.; Li, J.; Jia, C., *Anal. Methods* **2019,** *11* (17), 2311-2319.
13. Tang, Y.; Kong, X.; Xu, A.; Dong, B.; Lin, W., *Angew. Chem. Int. Ed.* **2016,** *55* (10), 3356-3359.
14. Wang, P.; Cheng, X.; Xiong, J.; Mao, Z.; Liu, Z., *Angew. Chem. Int. Ed.* **2022,** *40* (12), 1457-1463.
15. Chen, H.-W.; Li, H.; Song, Q.-H., *ACS Omega* **2018,** *3* (12), 18189-18195.
16. Ding, N.; Li, Z.; Hao, Y.; Zhang, C., *Anal. Chem.* **2022,** *94* (35), 12120-12126.
17. Wu, F.; Zhang, Y.; Huang, L.; Xu, D.; Wang, H., *Anal. Methods* **2017,** *9* (37), 5472-5477.
18. Wang, S.; Zou, Y.; Zhou, Y.; Hu, Y.; Yang, J.; Hou, Y.; Cheng, H., *Chem. Phys. Lett.* **2023,** *831*, 140846.
19. Wang, H.; Zhang, Y.; Rong, X.; Wang, B.; Wang, L.; Wang, C.; Gao, W.; Ye, X.; Hou, X.; Liu, W.; Wu, M.; Cheng, Y.; Shu, X.; Shang, J., *Spectrochim. Acta, Part A* **2024,** *313*, 124105.
20. Ding, N.; Li, Z.; Hao, Y.; Yang, X., *Food Chem.* **2022,** *384*, 132426.
21. Cao, T.; Gong, D.; Han, S.-C.; Iqbal, A.; Qian, J.; Liu, W.; Qin, W.; Guo, H., *Talanta* **2018,** *189*, 274-280.
22. He, L.; Yang, X.; Ren, M.; Kong, X.; Liu, Y.; Lin, W., *Chem. Commun.* **2016,** *52* (61), 9582-9585.
23. Liu, C.; Jiao, X.; He, S.; Zhao, L.; Zeng, X., *Dyes Pigm.* **2017,** *138*, 23-29.
24. Jana, A.; Joseph, M. M.; Munan, S.; K, S.; Maiti, K. K.; Samanta, A., *J. Photochem. Photobiol., B.* **2021,** *214*, 112091.
25. Cai, S.; Liu, C.; Gong, J.; He, S.; Zhao, L.; Zeng, X., *Spectrochim. Acta, Part A.* **2021,** *245*, 118949.
26. Jana, A.; Baruah, M.; Munan, S.; Samanta, A., *Chem. Commun.* **2021,** *57* (52), 6380-6383.
27. Xu, H.; Xu, H.; Ma, S.; Chen, X.; Huang, L.; Chen, J.; Gao, F.; Wang, R.; Lou, K.; Wang, W., *J. Am. Chem. Soc.* **2018,** *140* (48), 16408-16412.
28. Bi, A.; Liu, M.; Huang, S.; Zheng, F.; Ding, J.; Wu, J.; Tang, G.; Zeng, W., *Chem. Commun.* **2021,** *57* (28), 3496-3499.
29. Khosravi, A.; Moradian, S.; Gharanjig, K.; Afshar Taromi, F., *Dyes Pigm.* **2006,** *69* (1), 79-92.
30. Hojczyk, K. N.; Feng, P.; Zhan, C.; Ngai, M.-Y., *Angew. Chem. Int. Ed.* **2014,** *53* (52), 14559-14563.
31. Xu, A.; Tang, Y.; Lin, W., *Spectrochimica Acta Part A: Molecular and Biomolecular Spectroscopy* **2018,** *204*, 770-776.
32. Frisch, M. J.; Trucks, G. W.; Schlegel, H. B.; Scuseria, G. E.; Robb, M. A.; Cheeseman, J. R.; Scalmani, G.; Barone, V.; Mennucci, B.; Petersson, G. A.; Nakatsuji, H.; Caricato, M.; Li, X.; Hratchian, H. P.; Izmaylov, A. F.; Bloino, J.; Zheng, G.; Sonnenberg, J. L.; Hada, M.; hara, M.; Toyota, K.; Fukuda, R.; Hasegawa, J.; Ishida, M.; Nakajima, T.; Honda, Y.; Kitao, O.; Nakai, H.; Vreven, T.; Montgomery Jr., J. A.; Peralta, J. E.; Ogliaro, F.; Bearpark, M. J.; Heyd, J.; Brothers, E. N.; Kudin, K. N.; Staroverov, V. N.; Kobayashi, R.; Normand, J.; Raghavachari, K.; Rendell, A. P.; Burant, J. C.; Iyengar, S. S.; Tomasi, J.; Cossi, M.; Rega, N.; Millam, N. J.; Klene, M.; Knox, J. E.; Cross, J. B.; Bakken, V.; Adamo, C.; Jaramillo, J.; Gomperts, R.; Stratmann, R. E.; Yazyev, O.; Austin, A. J.; Cammi, R.; Pomelli, C.; Ochterski, J. W.; Martin, R. L.; Morokuma, K.; Zakrzewski, V. G.;Voth, G. A.; Salvador, P.; Dannenberg, J. J.; Dapprich, S.; Daniels, A. D.; Farkas, Ö.; Foresman, J. B.; Ortiz, J. V.; Cioslowski, J.; Fox, D. J. *Gaussian 09*, Gaussian, Inc.: Wallingford, CT, USA, **2009**.